# Raman and infrared studies of $La_{1-y}Sr_yMn_{1-x}M_xO_3$ ($M=$Cr, Co, Cu, Zn, Sc or Ga): Oxygen disorder and local vibrational modes

A. Dubroka*

*Materials Science Institute, University of Valencia, P.O. Box 22085, 46071 Valencia, Spain*
*and Institute of Condensed Matter Physics, Faculty of Science, Masaryk University, Kotlářská 2, CZ-61137 Brno, Czech Republic*

J. Humlíček

*Institute of Condensed Matter Physics, Faculty of Science, Masaryk University, Kotlářská 2, CZ-61137 Brno, Czech Republic*

M. V. Abrashev

*Faculty of Physics, University of Sofia, BG-1164 Sofia, Bulgaria*

Z. V. Popović,[†] F. Sapiña, and A. Cantarero

*Materials Science Institute, University of Valencia, P.O. Box 22085, 46071 Valencia, Spain*

We present results of our study of polarized Raman scattering and infrared reflectivity of rhombohedral ceramic $La_{1-y}Sr_yMn_{1-x}M_xO_3$ manganites in the temperature range between 77 and 320 K. In our samples, a part of the Mn atoms is substituted by $M=$Cr, Co, Cu, Zn, Sc, or Ga with $x$ in the range 0–0.1. The hole concentration was kept at the optimal value of about 32% by tuning the Sr content $y$. We have monitored distortions of the oxygen sublattice by the presence of broad bands in the Raman spectra, the increase of dc resistivity extracted from the infrared reflectivity, and the change of the critical temperature of the ferromagnetic transition. Our results support the idea that these properties are mainly determined by the radius of the substituent ion, its electronic and magnetic structure playing only a minor role. Furthermore, the Raman spectra exhibit an additional $A_g$-like high frequency mode attributed to the local breathing vibration of oxygens surrounding the substituent ion. Its frequency and intensity strongly depend on the type of the substituent. In the Co-substituted sample, the mode anomalously softens when going from 300 to 77 K. The frequency of the bulk $A_{1g}$ mode depends linearly on the angle of the rhombohedral distortion.

PACS number(s): 75.47.Lx, 78.30.−j, 63.20.Pw, 71.55.−i

## I. INTRODUCTION

Recently, considerable interest has been paid to $R_{1-x}A_xMnO_3$ manganites that are characterized by a strong interplay of spin, charge, and lattice degrees of freedom.[1] The research is motivated both by fundamental physical questions and by potential applications of the colossal magnetoresistance (CMR) appearing near the temperature of the ferromagnetic transition $T_c$. Much effort has also been devoted to the compounds $R_{1-y}A_yMn_{1-x}M_xO_3$ substituted at the Mn site. Substitutions of the Mn ion, which is at the heart of the double exchange (DE) interaction, may contribute to the knowledge of the basic mechanism of CMR and also allows one to tune the characteristics of the compounds such as $T_c$. Many researchers have addressed the transport and magnetic properties,[2–4] covering a wide range of materials with $R$=La, $A$=Ca, Sr, Ba and $M$=Al, Co, Cr, Cu, Fe, Ni, Sc, Ti, and Zn. The substitutions lead to a reduction of $T_c$ and magnetization, an increase of resistivity, and an enhancement of the magnetoresistance. In explaining these effects, a significant role has been attributed to the local elastic stress produced by the substituent and to its electronic and magnetic character. Only a few studies concerned the optical properties.[5–7]

In this paper we present results of polarized Raman scattering and an infrared reflectance study of ferromagnetic rhombohedral $La_{1-y}Sr_yMn_{1-x}M_xO_3$ compounds ($M=$Cr, Co, Cu, Zn, Sc, or Ga) for several concentrations of the substituent ($x$=0.02, 0.04, 0.06, 0.08, 0.1 for Cr, Co, Cu and Zn, $x$=0.1 for Sc and $x$=0.08 for Ga). In the compound, the substituents influence locally their surroundings and the average concentration of holes in the sample. In order to see more clearly the former effect, the concentration of holes has been kept approximately at 32% by adjusting the Sr content (see Sec. II). The presence or absence of broad bands around 500 and 620 cm⁻¹ in Raman spectra allows us to distinguish between strong and weak distortions of the oxygen sublattice. The distortions manifest themselves also in an increase of resistivity extracted from the infrared reflectivity. We discuss these effects and the variations of $T_c$ in terms of the radii of the substituents inferred from the x-ray data. We discuss in detail the properties of an additional $A_g$-like high-frequency peak found in Raman spectra. We investigate the relation of the frequency of the bulk $A_{1g}$ mode to the angle of the rhombohedral distortion.

The paper is organized as follows. In Sec. II we discuss the details of the experiments. In Sec. III A we comment on the results of x-ray analysis and variations of $T_c$. The main body of the paper (Sec. III B) is devoted to the Raman data. The results of the infrared studies are presented in Sec. III C and a summary in Sec. IV.

## II. SAMPLES AND EXPERIMENT

Polycrystalline, single phase $La_{1-y}Sr_yMn_{1-x}M_xO_3$ powders have been prepared by thermal decomposition of pre-

TABLE I. Compositions of the $La_{1-y}Sr_yMn_{1-x}M_xO_3$ samples.

| $La_{1-y}Sr_yMn_{1-x}M_xO_3$ | | | |
| --- | --- | --- | --- |
| $M$=Cu or Zn | | $M$=Cr, Co, Ga or Sc | |
| $x$ | $y$ | $x$ | $y$ |
| 0 | 0.30 | | |
| 0.02 | 0.274 | 0.02 | 0.294 |
| 0.04 | 0.248 | 0.04 | 0.288 |
| 0.06 | 0.222 | 0.06 | 0.282 |
| 0.08 | 0.196 | 0.08 | 0.276 |
| 0.10 | 0.170 | 0.10 | 0.270 |

cursors obtained by a freeze-drying of acetic acid solutions. This soft procedure makes possible a strict control of stoichiometry, and allows us to keep the concentration of vacancies at the La and Mn site practically negligible. Pellets were prepared by pressing and sintering the powder at 1150 °C for 48 h. The values of the parameters $x$ and $y$ were selected according to the valence of the substituent in order to maintain the constant proportion of $Mn^{4+}/Mn^{3+}$ ions of about 32%, see Table I. The valencies of the substituents were chosen as follows: $Sc^{3+}$ (the electron configuration $3d^0$), $Ga^{3+}$ ($3d^{10}$), and $Zn^{2+}$ ($3d^{10}$) ions are known to be the only possible states; the valencies of $Cr^{3+}$ ($3d^3$), $Co^{3+}$ ($3d^6$) ions are likely due to the charge neutrality condition. We have further assumed the valence state 2+ of Cu ($3d^9$) because the 3+ state is rare. However, it is not excluded that the actual valency of Cu is not integer and exceeds 2+. X-ray powder diffraction patterns were completely indexed with rhombohedral perovskite cells. For further details of the sample preparation and results of the diffraction analysis see Ref. 4. Table II presents the values of $T_c$ of our samples. The $La_{0.949}Mn_{0.949}O_3$ compound, which was prepared by the same procedure, was found to be a noncollinear ferromagnet with $T_c=145$ K.[8]

The Raman spectra were measured with a triple Jobin-Yvon 64000 spectrometer equipped with a liquid nitrogen cooled charge coupled device detector; the resolution was set to 2.7 cm$^{-1}$. The 488 nm Ar-Kr laser line was focused on a spot of a typical size of about 0.1 mm by a lens with the focal length of 10 cm, and collected in the pseudobackward

TABLE II. Values of $T_c$ (K) of our $La_{1-y}Sr_yMn_{1-x}M_xO_3$ samples, taken from Ref. 4.

| | $x$ | | | | | |
| --- | --- | --- | --- | --- | --- | --- |
| $M$ | 0 | 0.02 | 0.04 | 0.06 | 0.08 | 0.10 |
| Cr | 372 | 363 | 351 | 340 | 327 | 316 |
| Co | | 355 | 345 | 331 | 312 | 300 |
| Cu | | 358 | 331 | 308 | 274 | 236 |
| Zn | | 350 | 326 | 284 | 233 | 179 |
| Sc | | | | | | 195 |
| Ga | | | | | 320 | 310 |

scattering geometry. The power of the laser at the sample was kept below 18 mW. From the frequency shift of the soft mode around 200 cm$^{-1}$ we have estimated that the overheating of the spot on the sample was less than 10 K. Samples were cooled using a continuous flow cryostat.

Raman signals from polycrystalline samples have been collected in the macro regime from a number of randomly oriented microcrystals because the spot of the light is much larger than the typical size of the microcrystals of about 1 $\mu$m. We have performed polarized measurements in two scattering geometries with parallel ($e_i \| e_s$) and crossed ($e_i \perp e_s$) polarizations of the incident and the scattered light, respectively. Although we are not able to extract individual components of the Raman tensor, these two geometries have different selection rules for the Raman lines, providing more information than unpolarized measurements. To get rid of the trivial temperature dependence, all spectra have been divided by the Bose-Einstein occupation number $n(\omega)+1=1/[1-\exp(-\hbar\omega/k_BT)]$.

The infrared reflectivity was measured in the range 80–7000 cm$^{-1}$ using a Bruker IFS 66v/S spectrometer. The samples were cooled using a Janis ST-100-FTIR continuous flow cryostat.

## III. RESULTS AND DISCUSSION

### A. X-ray data and $T_c$

An insight into the differences among the substituents can be obtained by analyzing the x-ray data.[4] A particularly important information is provided by the $B$-O distance, i.e., the mean distance between the central ion in the perovskite $AB$O$_3$ structure and neighboring oxygens. In the case of the 10% substituted samples, this quantity represents the average of nine Mn-O distances and one $M$-O distance. Since the average valency of the Mn ions is kept constant and their radius is thus fixed, the $B$-O distance should depend on the radii of the $M$ ions. Figure 1(a) displays the volume of the elementary cell versus the $B$-O distance. It is apparent that the compounds can be sorted into two groups according to the $B$-O distance: (i) close to that of the parent compound (Cr, Co, and Ga), and (ii) significantly larger (Sc, Zn, and Cu). This indicates that the radii of the substituents within the former (latter) group are similar to (larger than) the radius of the Mn ion. This differentiation can also be noted in the variations of the volume of the elementary cell. The volume, however, is a quite complex quantity. For example, a decrease of the volume of the $La_{1-y}Sr_yMnO_3$ system with increasing concentration of Sr (Ref. 9) contradicts a simple expectation based only on the Shannon radii of La and Sr (that of Sr is larger). The observed trend is probably caused by the increase of the concentration of the $Mn^{4+}$ ions that are smaller than the $Mn^{3+}$ ions. In our samples, where the concentration of holes is kept constant, the variations of the volume can thus be expected to follow predominantly those of the substituent radii. However, the volume of Cu- and Zn-substituted samples is lower than that of the Sc-substituted sample due to a higher concentration of Sr in the latter. The inset of Fig. 1(a) displays the $B$-O distance of
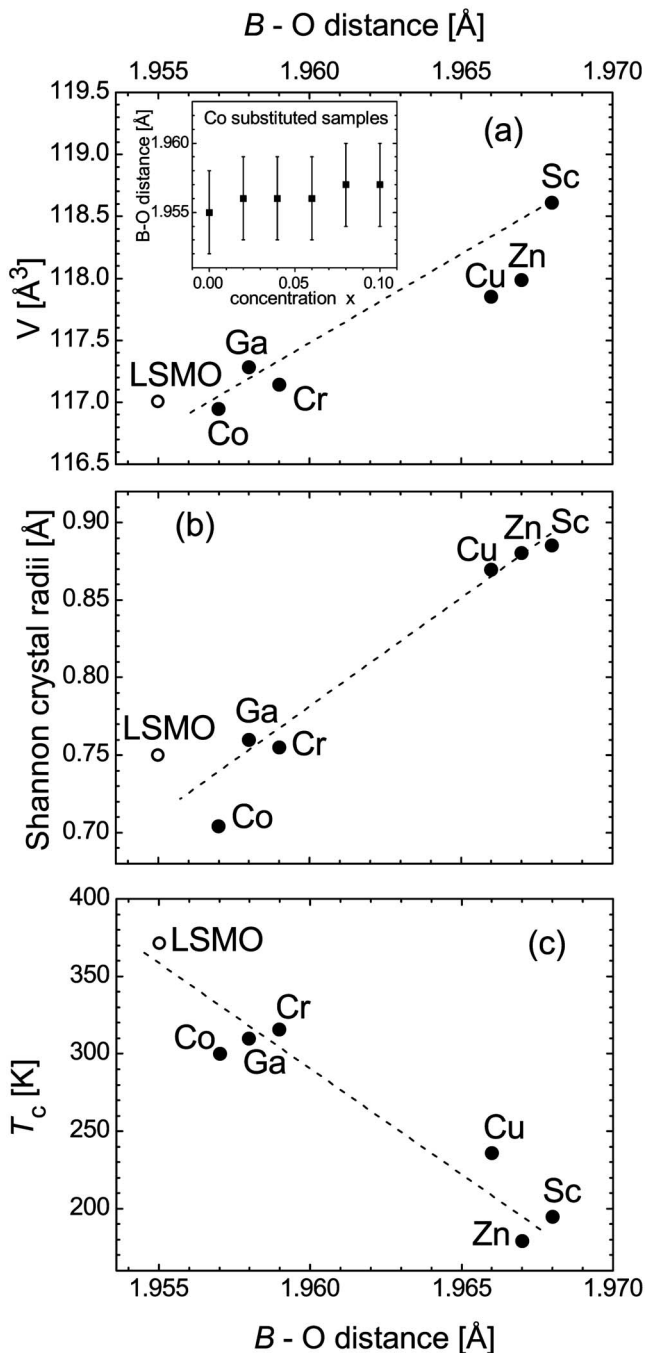
FIG. 1. Volume of the elementary cell (a), Shannon radius of the substituents (b), and $T_c$ (c), versus the $B$-O distance of the $La_{1-y}Sr_yMn_{1-x}M_xO_3$, $x=0.10$ samples and the parent $x=0$ (LSMO) sample. X-ray data are taken from Ref. 4. The dashed lines are shown to guide the eye. The inset of the part (a) displays the $B$-O distance of the Co-substituted samples.

Co-substituted samples as the function of the concentration $x$ including error bars corresponding to the standard deviation of 0.003 Å resulting from x-ray analysis.[4] Obviously, the dispersion of experimental points is much lower than 0.003 Å, our estimate is about 0.001 Å. Because of this difference, we do not display the error bars of the $B$-O distance in our figures. Since the present paper is focused mainly on the

distinction between the groups of samples (i) and (ii), the conclusions will not be influenced even by the error margin of 0.003 Å. A similar discrepancy between the nominal standard deviation and the real dispersion of data points is apparent in Fig. 1 of Ref. 10.

The values of the $B$-O distance are compared with the Shannon radii[11] in Fig. 1(b); the latter correspond to the valence of 3+ for Sc, Cr, Co, and Ga ions, and 2+ for Cu and Zn ions. For Co, we have used the value of the intermediate spin state that is estimated to be about 3% larger than that of the low spin state.[12] The radius of Mn was calculated as the weighted average of those of the $Mn^{3+}$ and $Mn^{4+}$ ions, for the mean oxidation state of 3.3. The Shannon radius correlates reasonably well with the $B$-O distance, supporting the relevance of the representation of the substituent radii by the $B$-O distance. Moreover, the $B$-O distance seems to be essentially independent of the Sr concentration. For example, the values for the Zn and Sc points corresponding to the Sr content of 0.17 and 0.27, respectively, are almost the same.

Figure 1(c) displays $T_c$ versus the $B$-O distance. A pronounced reduction of $T_c$ occurs for Cu-, Zn- and Sc-substituted samples, where the radius of the substituent is larger than that of the Mn ion. This correlation has been attributed to a modification of the Mn-O distances around the substitutional ion,[2] leading to changes of the energies of the $e_g$ orbitals [similar to those of the Jahn-Teller (JT) effect], and to a localization of the itinerant electrons that reduces the DE interaction and $T_c$.

### B. Raman scattering

Our samples crystallize in rhombohedral structure, space group $D_{3d}^6$, $Z=2$. This structure can be obtained from the simple cubic perovskite by the rotation of the adjacent $MnO_6$ octahedra in the opposite directions around the $[111]_c$ cubic direction. Of the total of the 20 $\Gamma$-point modes ($A_{1g}+3A_{2g}+2A_{1u}+4A_{2u}+4E_g+6E_u$), five ($A_{1g}+4E_g$) are Raman active, eight ($3A_{2u}+5E_u$) are infrared active, and five ($2A_{1u}+3A_{2g}$) are silent.

Figure 2(a) shows our Raman spectra of the parent compound $La_{0.7}Sr_{0.3}MnO_3$ at 77 and 300 K. The low temperature spectrum measured in the $e_i\|e_s$ polarizations exhibits three lines at 200, 427, and 663 cm$^{-1}$. The shell model calculation of the isostructural rhombohedral $LaMnO_3$ from Ref. 13 predicts the frequency of the $A_{1g}$ mode of 249 cm$^{-1}$ and the frequencies of $E_g$ modes at 42, 163, 468, and 646 cm$^{-1}$. Similarly to previous studies,[13–15] we assign the 200 cm$^{-1}$ line to the $A_{1g}$ mode, and the 427 cm$^{-1}$ line to the $E_g$ mode with the predicted frequency of 468 cm$^{-1}$. This assignment is supported by the different symmetry of the modes that is apparent in the $e_i\perp e_s$ spectrum, where only the $E_g$ mode is present. The frequencies of the two modes are close to the results obtained on a single crystal (199 and 426 cm$^{-1}$, respectively,[14]). In all our spectra, the $E_g$ mode has almost the same frequency, 427±2 cm$^{-1}$ at 77 K, and it softens slightly with increasing temperature. We do not assign the weak band at 663 cm$^{-1}$ to the manganite because its intensity varies substantially from measurement to measurement. Similarly to Podobedov et al.,[15] we assume that it is due to a
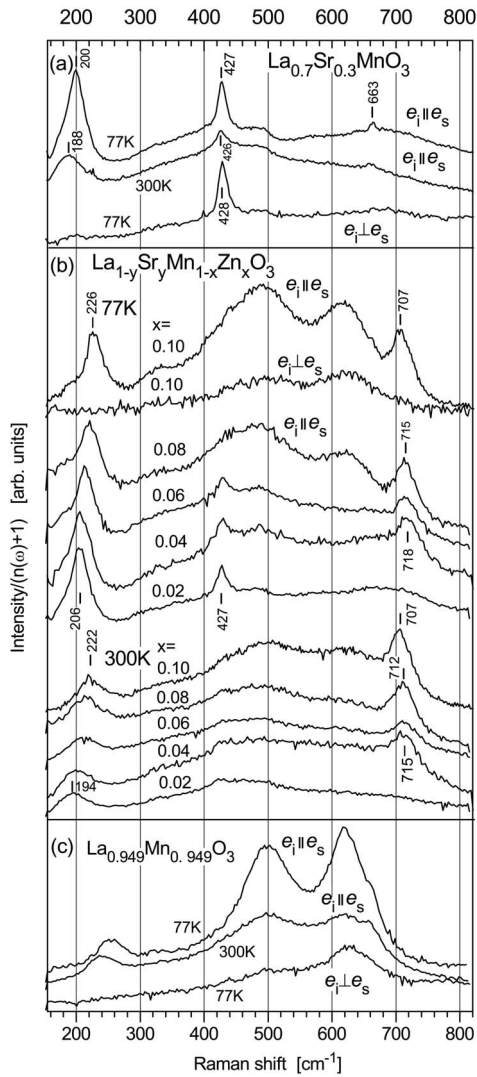
FIG. 2. Raman spectra of (a) $La_{0.7}Sr_{0.3}MnO_3$, (b) $La_{1-y}Sr_yMn_{1-x}Zn_xO_3$, and (c) $La_{0.949}Mn_{0.949}O_3$ polycrystalline samples measured for the parallel polarizations of the incident and the scattered light. The spectra measured for the crossed polarizations are marked by $e_i \perp e_s$.



FIG. 3. Raman spectra of polycrystalline $La_{1-y}Sr_yMn_{1-x}Cu_xO_3$ samples. All spectra were measured for parallel polarizations of the incident and the scattered light except for the spectrum of the $x$ =0.10 sample, marked by $e_i \perp e_s$, which was measured for the crossed polarizations.

small volume of manganese oxides, e.g., $Mn_3O_4$ has a strong Raman line at about this frequency.[16]

Figure 2(b) shows the Raman spectra of the Zn-substituted series. With increasing Zn concentration, the spectra exhibit the following main features: the $A_{1g}$ mode hardens, a fairly strong mode appears at about 710 cm$^{-1}$, the mode at 427 cm$^{-1}$ gradually disappears while two broad bands appear at 500 and 620 cm$^{-1}$. The broad bands are discussed in Sec. III B 1.

Figures 3–5 display the Raman spectra of the Cu, Cr, and Co series, respectively. First, let us focus on the 77 K spectra measured in the $e_i \| e_s$ polarizations. With increasing concentration of the substituent, the oxygen bending mode at 427 cm$^{-1}$ weakens but remains well resolved even at the largest concentration of $x$=0.10. However, even at the highest $x$ none of the spectra exhibits the broad bands such as in the Zn-substituted series. A high-frequency mode emerges at
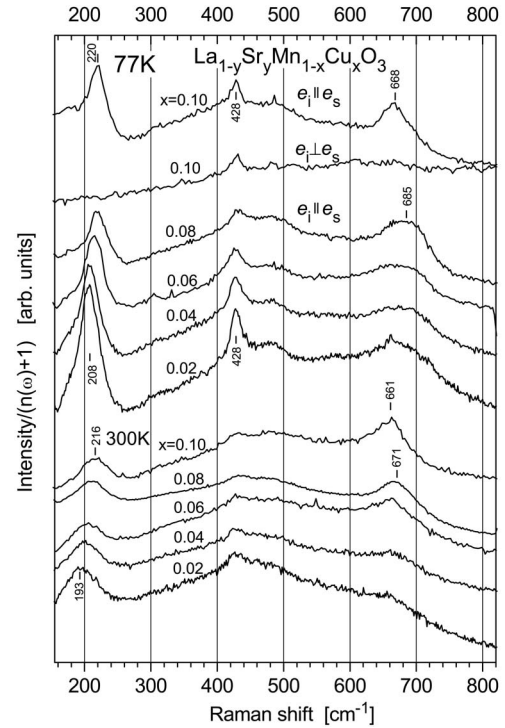
about 670 cm$^{-1}$ (Cu), 728 cm$^{-1}$ (Cr), and 644 cm$^{-1}$ (Co), respectively. The mode is discussed in detail in Sec. III B 2. The low-frequency $A_{1g}$ mode hardens with increasing concentration of substituents, which will be discussed in Sec. III B 3. We have performed temperature studies (not shown) between 300 and 77 K of several selected samples (Zn 10%, Zn 6%, Cu 10%, Cu 8%, Cr 4%, and Co 2%). The spectra exhibit basically a gradual change between 300 and 77 K.

Figure 6 summarizes the 77 K spectra of the $x$=0.10 compounds including the one of Sc, which exhibits broad bands similar to those of the Zn sample and a high-frequency peak at 759 cm$^{-1}$. The 77 K spectrum of the Ga $x$=0.08 sample is shown as well. A Ga-substituted sample with $x$=0.10 was not available for our optical studies; however, we expect the difference between the samples with Ga concentration of 0.10 and 0.08 to be rather small and the absence of this particular composition does not degrade our qualitative conclusions. In the spectrum of the Ga sample, there is no pronounced line at high frequencies; however, it is possible that a high-frequency mode similar to those of the remaining samples is present as the weak structure around 720 cm$^{-1}$.

### 1. Jahn-Teller-like bands

As far as the broad bands are concerned, the spectra displayed in Fig. 6 can be divided into two groups: that of the Zn- and Sc-substituted samples displaying them, and that of Cu-, Cr-, Co-, and Ga-substituted samples where they are absent. Spectral structures very similar to these broad bands
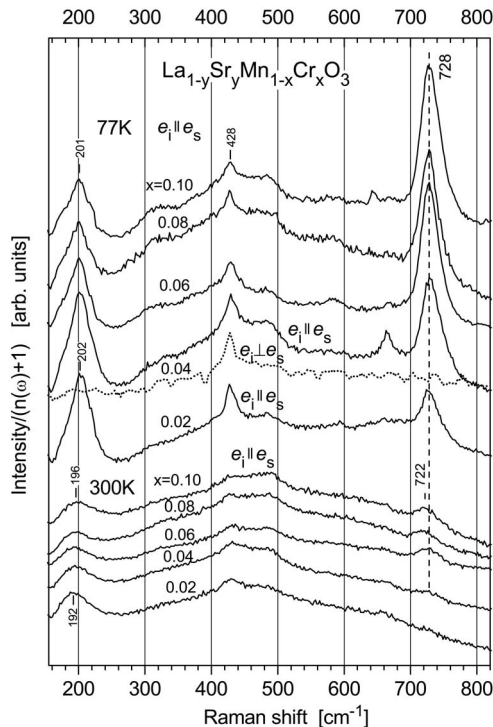
FIG. 4. Raman spectra of polycrystalline $La_{1-y}Sr_yMn_{1-x}Cr_xO_3$ samples. All spectra were measured for parallel polarizations of the incident and the scattered light except for the spectrum of the $x=0.04$ sample, marked by $e_i \perp e_s$, which was measured for the crossed polarizations.



FIG. 5. Raman spectra of polycrystalline $La_{1-y}Sr_yMn_{1-x}Co_xO_3$ samples. All spectra were measured for parallel polarizations of the incident and the scattered light except for one spectrum of the $x=0.10$ sample, marked by $e_i \perp e_s$, which was measured for the crossed polarizations. The inset shows the frequency of the $A_g$-like mode of the $x=0.02$ sample versus temperature.

were observed in the paramagnetic phase of $La_{0.7}Ca_{0.3}MnO_3$ (Ref. 17) and $La_{0.8}Sr_{0.2}MnO_3$,[18,19] disappearing in the ferromagnetic metallic phase. These structures ("JT bands") have been assigned to the scattering on the oxygen sublattice distorted by the JT effect.[20] The JT distortion is not compatible with the rhombohedral structure where all Mn-O bonds have equal length, and results in a noncoherently distorted oxygen sublattice. Raman scattering on such structures is not restricted by selection rules and its intensity is proportional to the phonon density of states.[21] The disappearance of the bands in the metallic phase corresponds to a decrease of JT distortions due to the delocalization of the $e_g$ electrons.

We suggest that the broad bands in the Zn- and Sc-substituted compounds are also caused by distortions of the oxygen sublattice. In these samples, however, the distortions are primarily induced by the substituents; consequently, we call the broad bands JT-like bands rather than JT bands. The intensity of the JT-like bands obviously increases with the concentration of the substituents. The appearance of the JT-like bands correlates with the $B$-O distance (or, equivalently, with the radius of the substitutional ion): they are present in the spectra of Sc- and Zn-substituted compounds (large radii) and absent in Cr-, Co-, and Ga-substituted samples (small radii). The JT-like bands are not observed in the Cu-substituted compounds, indicating a weaker oxygen disorder than in the Zn and Sc series, although the substitutional ions have comparable radii.

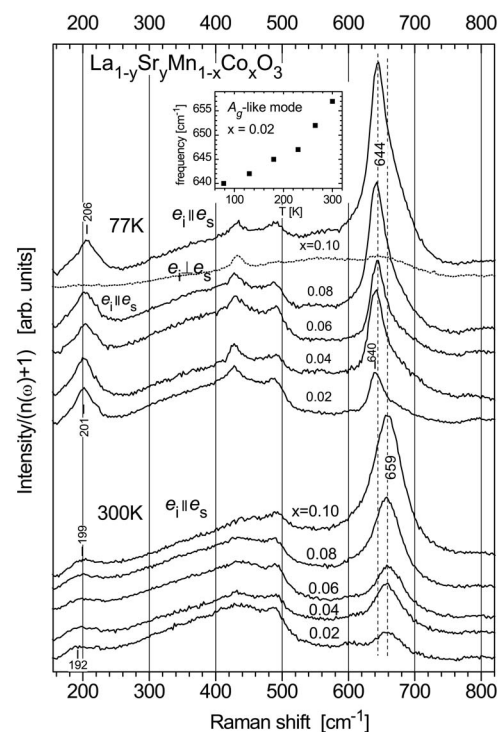It is possible that the distortion of the oxygen sublattice results from two distinct steps: first, the oxygens neighboring to the substitutional ions are displaced directly by the stress produced by the substituent. Secondly, this displacement can lead to a localization of the $e_g$ electrons around the substitutional ion, stimulating an additional long-range distortion of the oxygen sublattice by the JT effect. This additional distortion can be enhanced by electronic and magnetic properties of the substituent, e.g., the impossibility of acquiring the $e_g$ electron in the case of $3d^{10}$ electron configurations of the substituent, a magnetic state of the substituent that weakens the ferromagnetism, etc. The suggestion of a long-range distortion involving oxygens farther from the substituent is supported by the fact that the frequency and the width of the broad bands does not differ between Sc- and Zn-substituted compounds and $La_{0.949}Mn_{0.949}O_3$ [see Fig. 2(c)]. This is in contrast with the local vibrational modes (see Sec. III B 2) that depend strongly on the type of substituent. The secondary distortion can be the reason why the Cu-substituted series differs from the Zn- and Sc-substituted ones. It is possible that the electronic and magnetic structure of Cu ions does not support the localization of the $e_g$ electrons and the related second step of the distortions. We discuss further this topic in Sec. III C.

The JT-like bands of Zn- and Sc-substituted samples persist in the ferromagnetic phase (see Fig. 6) since they originate primarily from the distortions of the oxygen sublattice induced by the substituents. This trend is in contrast with the observations, e.g., in $La_{0.8}Sr_{0.2}MnO_3$,[19] where the broad bands are caused by JT distortions and both the JT distor-

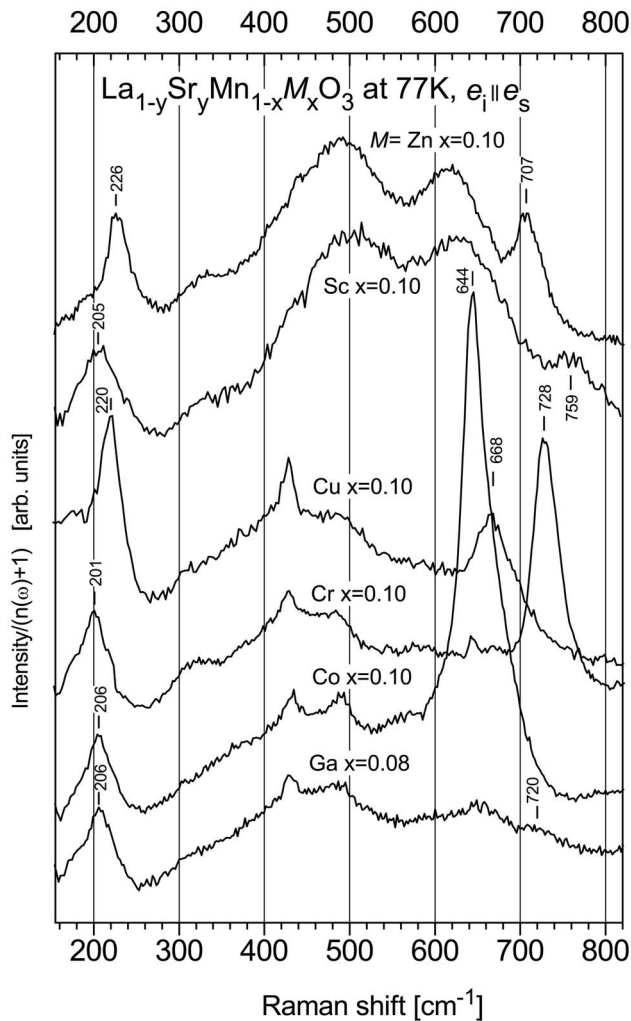FIG. 6. Raman spectra of $La_{1-y}Sr_yMn_{1-x}M_xO_3$, $x=0.10$, samples (except for $M=$Ga with $x=0.08$) measured for parallel polarizations of the incident and the scattered light.



FIG. 7. The frequency of the additional $A_g$-like mode as a function of the atomic number.

tions and the broad bands are suppressed in the ferromagnetic phase. Actually, the JT-like bands are more pronounced at 77 K than at 300 K [see Fig. 2(b)]. This is probably due to a reduction of the width of the bands resulting from an increase of the lifetime of the corresponding vibrational states with decreasing temperature.[22]

The broad bands are also present in the $La_{0.949}Mn_{0.949}O_3$ sample [see Fig. 2(c)]. This sample is doped by vacancies and contains 35% of $Mn^{4+}$ ions. The high concentration of vacancies at the Mn site (5.1%), however, transforms the low temperature phase into a resistive noncollinear ferromagnet.[8] Consequently, the distortions of the oxygen sublattice and the broad bands persist also below $T_c$. The broad bands with similar temperature evolution were observed also in a $La_{0.7}Ca_{0.3}MnO_3$ sample.[23]

### 2. The additional $A_g$-like high-frequency mode

Let us discuss the peak observed at the highest frequencies of $640-760$ $cm^{-1}$. Its common characteristics are (a) it appears only in Mn-substituted samples and its intensity in-
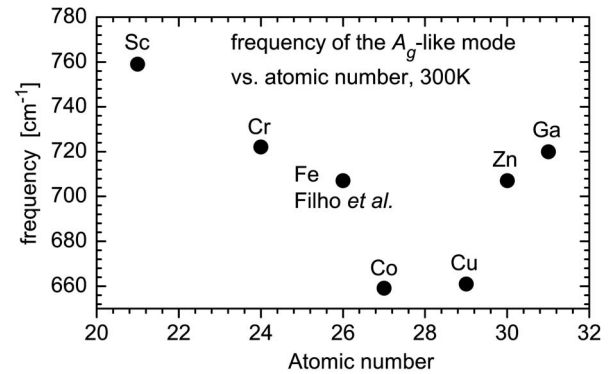
creases with the concentration of substituents (the increase is most pronounced in the Cr and Co series), (b) it has $A_g$-like properties: it is absent or strongly suppressed in the $e_i \perp e_s$ spectra, (c) in contrast to the JT-like bands, it has a relatively small spectral width, (d) its frequency depends rather strongly on the type of the substituent. We assign the peak to a local breathing (in-phase stretching) mode of oxygens in a close vicinity of the substituent ion. This interpretation is further supported by the symmetry of the mode: the suggested eigenvector corresponds to a nondegenerate vibration, i.e., it has the $A_g$-like symmetry. Moreover, these modes are not infrared active (see Sec. III C) which implies that the eigenvector should have a center of symmetry. The property (c) indicates that the peak does not originate from the phonon density of states. Filho *et al.*[7] observed a similar peak at about 707 $cm^{-1}$ in $La_{0.70}Sr_{0.30}Mn_{1-x}Fe_xO_3$ and interpreted it as the silent $A_{2g}$ mode activated by a symmetry breaking or as the phonon density of state feature. However, this interpretation is in contradiction with the property (d).

Figure 7 summarizes the frequencies of the additional $A_g$-like mode including the Fe data of Ref. 7. Evidently, the frequency does not exhibit a simple mass effect. This is not surprising, because the substitutional ions do not take part in the vibration. The data do not indicate a simple monotonic relation between the frequency and the $B$-O distance. Some other factor than the radius of the substituents must play an important role. It could be, e.g., the degree of covalency of the $M$-O bond, which would imply a dependence of the frequency on the position of $M$ atom in the Periodic Table. Indeed, it can be seen in Fig. 7 that the frequency decreases when going from the borders of the group of transition metals, where the covalency can be supposed to be small, towards the center, where it should be larger. Surprisingly, the intensity of the peak exhibits the same trend: in Co-substituted compounds the intensity is the largest and it is very small in Sc- and Ga-substituted compounds. The peak of the Fe-substituted compound observed in the data of Filho *et al.*[7] has also a very large intensity as compared with the other phonons. Another factor affecting this frequency can be the valence of the substituent that influences electrostatically the stiffness of the $M$-$O^{2-}$ bond. This effect would lower the frequencies corresponding to the substituents with valencies 2+ (Cu and Zn) with respect to their hypothetical 3+ state.

However, a clear understanding of the frequency and intensity variations remains a challenge for future studies.

The properties of the high-frequency mode are even more complex. In the Co series, the mode anomalously softens by about 15 cm$^{-1}$ with decreasing temperature, and becomes rather asymmetric at 77 K. It is possible that this anomaly is due to the transition from the intermediate spin state occurring at room temperature, to the low spin state at low temperature.[12] These two states differ in electronic configuration as well as in ionic radius, which could influence the frequency as discussed above. The frequency increases steeply in the temperature range between 200 and 300 K (see the inset of Fig. 5) and we expect that it will continue to increase considerably above 300 K, where Co passes into the high spin state.[12] In the Cu-substituted samples with $x$ =0.04, 0.06, 0.08, the mode appears to consist of a peak at 660–670 cm$^{-1}$ present both at room and at low temperature, and a peak at about 690–700 cm$^{-1}$ emerging at low temperature. The two frequencies are likely to correspond to two types of Cu-O bonds with different stiffnesses. The difference in bonding can be caused, e.g., by the reduction of the cubic symmetry of the $CuO_6$ octahedra due to the JT effect. The frequency of the mode of Zn- and Cu-substituted samples with $x$=0.10 is considerably lower (about 9 cm$^{-1}$) than that of the $x$=0.08 samples. This can be a consequence of an interaction between the areas around the substituent ions, that must increase with increasing concentration.

### 3. The $A_{1g}$ soft mode

The $A_{1g}$ mode of the rhombohedral structure has the frequency within the interval 190–220 cm$^{-1}$. The vibrational pattern of this mode has the shape of the rhombohedral distortion[13] (static rotational displacement of the oxygen octahedra around the cubic [111] direction). With increasing temperature towards the transition from rhombohedral to cubic structure at about 800 °C,[24] its frequency should decrease to zero, i.e., it is a soft mode. In our spectra, in accord with this interpretation, the $A_{1g}$ mode hardens when going from 300 to 77 K. In the parent compound $La_{0.7}Sr_{0.3}MnO_3$, the hardening is about 12 cm$^{-1}$ in good agreement with the results of Ref. 15; in the spectra of the substituted samples, the frequency change is weaker. As noted by Abrashev *et al.*,[13] based on the form of the eigenvector of the $A_{1g}$ mode, its frequency should mainly correlate with the angle $\alpha$ of the rhombohedral distortion. The angle can be calculated from the coordinate $x_O$ of the oxygens [$(x_O, 0, 1/4)$ in a hexagonal setting] by using this equation[25]

$$x_O = \frac{1}{2}\left(1 \pm \frac{1}{\sqrt{3}} \tan \alpha\right). \quad (1)$$

Figure 8 shows the dependence of the frequency of the $A_{1g}$ mode on $\alpha$, the values of the latter quantity being calculated from those of the $x_O$ (Ref. 7) (see the inset of Fig. 8). The frequency is almost a linear function of $\alpha$, and falls on
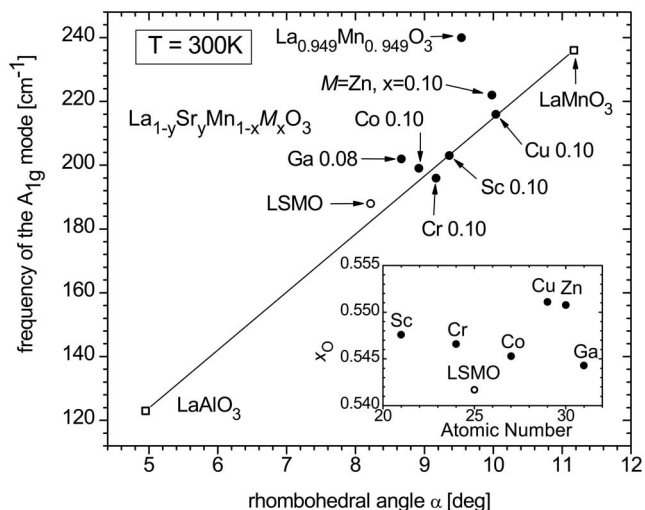


FIG. 8. Frequency of the $A_{1g}$ soft mode versus the angle of rhombohedral distortion $\alpha$ of the $La_{1-y}Sr_yMn_{1-x}M_xO_3$ samples and the parent $x$=0 (LSMO) sample. The data for $LaMnO_3$ and $LaAlO_3$ taken from Ref. 13 are connected by the straight line. The inset shows the values of the coordinate $x_O$ of the oxygens versus the atomic number.

the line connecting the data for $LaMnO_3$ and $LaAlO_3$ of Ref. 13. The angle $\alpha$ is influenced mainly by the Sr content $y$, putting the Cu and Zn points apart from the other compounds. The radius of the substituted ions seems to play only a minor role. For example, the values of the frequency and $\alpha$ for Sc and Co, Cr, Ga are very similar, in spite of a significantly larger radius of Sc compared to the remaining ions. The only outlier is the $La_{0.949}Mn_{0.949}O_3$ ($x_O$=0.5485 Å taken from Ref. 26). Since it is the only compound among our samples that has a significant concentration of vacancies, we attribute the deviation to this structural difference. The linear dependence of the frequency of the octahedra tilt mode on the tilt angle has been found also in orthorhombic manganites.[27]

### C. Infrared reflectance

Figure 9 presents the measured infrared reflectivities of the $x$=0.10 samples (including the Ga-substituted sample with $x$=0.08). In order to compare the samples in the same magnetic state, the spectra were measured at the critical temperature of each compound. In the region from 130 to 600 cm$^{-1}$ the spectra exhibit several phonon structures reported already in earlier studies.[6] No phonon modes are observed (within the noise ⩽0.1%) in the frequency region of the additional $A_g$-like Raman lines (640–800 cm$^{-1}$). This excludes the possibility that the Raman lines are due to infrared phonons activated by a reduction of symmetry. In the following, we focus on the long-wavelength behavior of the itinerant electrons, and extract the dc resistivity. We recall that the dc resistivity of a polycrystal determined from the infrared spectroscopy is likely to be closer to the intrinsic
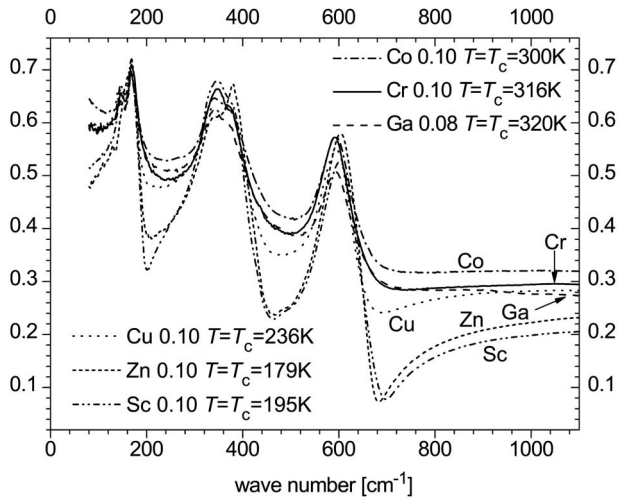
FIG. 9. Infrared reflectivities of the $La_{1-y}Sr_yMn_{1-x}M_xO_3$, $x=0.10$ compounds (except for $M=$Ga with $x=0.08$) measured at the critical temperatures of each sample.

resistivity than the data obtained by standard transport measurements because it is much less sensitive to the intergrain boundaries.[28] Already the raw reflectivity data of the Zn- and Sc-substituted samples can be seen to differ from the others by a lower background and more pronounced phonon structures, which corresponds to a higher dc resistivity. In order to explore the difference quantitatively, we have fitted the spectra using the model dielectric function in the standard form of a sum of Lorentzian oscillators,

$$\epsilon(\omega) = \epsilon_\infty - \frac{F_D}{\omega(\omega + i\gamma_D)} + \sum_j \frac{F_j}{\omega_j^2 - \omega^2 - i\omega\gamma_j}, \quad (2)$$

where $\epsilon_\infty$ stands for the electronic interband contribution, the second term is the contribution of the conduction electrons, and the sum represents phonons. Normal incidence reflectivity was calculated as $R=|(1-N)/(1+N)|^2; N=\sqrt{\epsilon}$. We have fitted the data in the interval 80–1500 cm$^{-1}$. This region is sufficient to yield a reasonable description of the behavior of the conducting electrons, keeping a simple model with a small number of parameters, which would be impossible when including higher frequencies. The fitted reflectance spectra and the resulting real part of the complex conductivity, $\sigma(\omega)=-i\omega\epsilon_0\epsilon(\omega)$, are plotted in Fig. 10. The agreement between the data and fits is reasonable; resulting values of the parameters are shown in Table III.

Figure 11 shows the values of the dc resistivity, $\rho=1/\mathrm{Re}\,\sigma(\omega=0)$. The trend of increasing resistivity with increasing $B$-O distance is clearly visible; the values corresponding to the large substituents, Sc and Zn, are significantly larger than those of the smaller ones. The resistivity of the Cu-substituted compound is close to that of the group of smaller substituents. This is the same trend as indicated by the JT-like bands in the Raman data.

We explain the difference between the Cu- and Zn-substituted compound in terms of the occupancy of the $3d$ orbitals as follows: the Zn$^{2+}$ ion has fully occupied $3d$ orbitals in contrast with the Cu$^{2+}$ ion, that has one $3d$ orbital empty. This orbital can acquire a conduction electron, and creates a nonzero magnetic moment that might enhance the
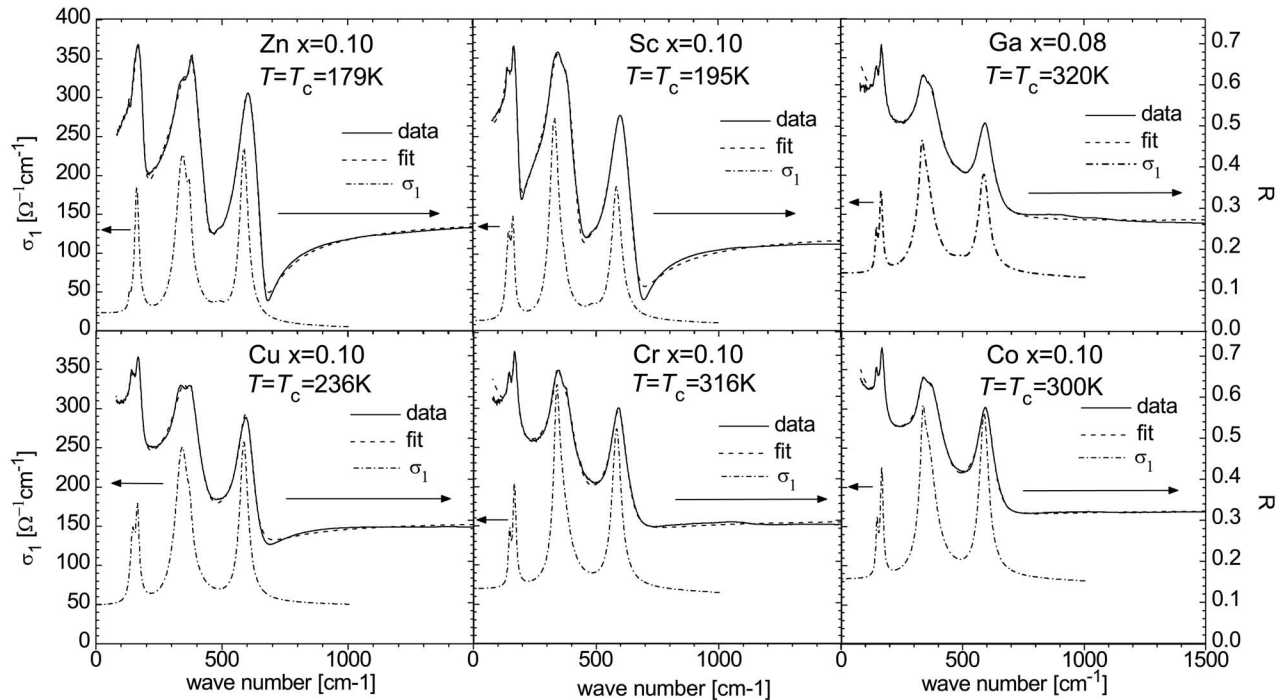


FIG. 10. Infrared reflectivities of Fig. 9 (solid lines) with fits (dashed lines) and the real part of complex conductivity (dash-dotted lines). The reflectivities and the conductivities correspond to the right and left axes, respectively.

TABLE III. Best-fit values of the parameters of the dielectric function (2). The units of $F_j$ are $10^3$ cm$^{-2}$, the units of $\omega_j$ and $\gamma_j$ are cm$^{-1}$. The error of the dc resistivity $\rho(\omega=0)=\gamma_D/(\epsilon_0 F_D)$ is about 10%, however, the errors of $F_D$ and $\gamma_D$ itself are large due to the flat conductivity background in the FIR region. The errors of the remaining values are a few percent except for the widths and strengths of the overlapping phonons at 340 and 370 cm$^{-1}$, where the uncertainty is about 50%.

| | Zn 10% | Sc 10% | Ga 8% | Cu 10% | Cr 10% | Co 10% |
|---|---|---|---|---|---|---|
| $\epsilon_\infty$ | 10.2 | 8.7 | 11.3 | 12.1 | 12.9 | 14.5 |
| $F_D$ | 576 | 1400 | 13400 | 16200 | 12600 | 19600 |
| $\gamma_D$ | 411 | 1505 | 3000 | 5380 | 3000 | 3917 |
| $F_1$ | 5 | 146 | 29 | 112 | 41 | 42 |
| $\omega_1$ | 131 | 146 | 146 | 145 | 147 | 147 |
| $\gamma_1$ | 6 | 23 | 10 | 22 | 11 | 11 |
| $F_2$ | 204 | 82 | 93 | 100 | 118 | 113 |
| $\omega_2$ | 160 | 164 | 166 | 164 | 167 | 166 |
| $\gamma_2$ | 20 | 13 | 15 | 16 | 15 | 13 |
| $F_3$ | 784 | 686 | 66 | 765 | 323 | 140 |
| $\omega_3$ | 341 | 332 | 333 | 340 | 339 | 335 |
| $\gamma_3$ | 63 | 45 | 20 | 65 | 28 | 23 |
| $F_4$ | 53 | 51 | 615 | 46 | 438 | 726 |
| $\omega_4$ | 370 | 370 | 346 | 371 | 362 | 357 |
| $\gamma_4$ | 15 | 40 | 80 | 21 | 75 | 77 |
| $F_5$ | 25 | 20 | 15 | | | |
| $\omega_5$ | 488 | 487 | 485 | | | |
| $\gamma_5$ | 50 | 50 | 50 | | | |
| $F_6$ | 540 | 488 | 381 | 488 | 543 | 571 |
| $\omega_6$ | 586 | 586 | 587 | 585 | 583 | 587 |
| $\gamma_6$ | 40 | 48 | 51 | 40 | 45 | 46 |

ferromagnetism. However, the Ga$^{3+}$ ion has the 3$d$ shell occupied and has no magnetic moment, but the samples belong to the low resistivity group. The Ga substitution shows that the structural and electric properties of the compounds are mainly related to the substituent radius, and can be partially influenced by its electronic and magnetic structure; this seems to be the case in the Cu-substituted compound.

Alonso *et al.*[29] suggested that an important factor influencing magnetic properties of the substituted manganites is the electrostatic potential created by the substituent. In this picture, because the average valence of the Mn ions is 3.3+, holes are attracted to the substituent with a lower valence (3+ or 2+), and, consequently, the holes tend to localize and $T_c$ decreases. If this effect were important, the $T_c$ of the Zn$^{2+}$-substituted sample would be significantly lower than that of the Sc$^{3+}$-substituted compound, because the valence 2+ should localize holes more strongly than the valence 3+. In our samples, however, the $T_c$'s of these compounds are nearly the same. This fact indicates that the influence of the electrostatic potential on the localization of holes is significantly less important than that of the local pressure.

Ghosh *et al.*[2] studied the effects of Mn substitutions by transition elements in La$_{0.7}$Ca$_{0.3}$MnO$_3$. It has been found that the changes of the maximum of magnetoresistance correlate



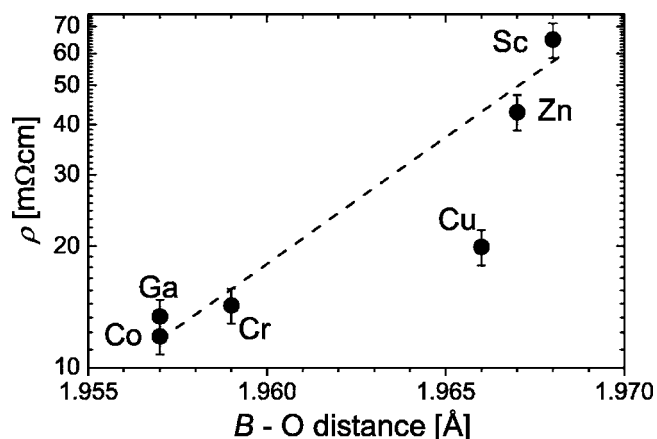FIG. 11. The values of the dc resistivity of the La$_{1-y}$Sr$_y$Mn$_{1-x}$M$_x$O$_3$, $x=0.10$ compounds (except for $M=$Ga with $x=0.08$) extrapolated from the infrared data. The dashed line is shown to guide the eye.

with those of the lattice parameter, and that $T_c$ correlates with the conductivity at $T_c$. The latter result is basically confirmed by our studies.

## IV. SUMMARY AND CONCLUSIONS

We have used Raman and infrared spectroscopy, magnetic measurements, and x-ray analysis to study the influence of Mn-site substitutions in optimally doped manganites. Our results support the idea that the main factor influencing the oxygen disorder and electric and magnetic properties of these compounds is the radius of the substituents and that their electronic and magnetic structure plays only a minor role. Our substituents form two groups, with the radii significantly larger than (Zn$^{2+}$ and Sc$^{3+}$), and similar to (Co$^{3+}$, Cr$^{3+}$, Ga$^{3+}$), the average radius of the Mn ions. The former group differs from the latter by the occurrence of JT-like bands in the Raman spectra, reflecting an enhanced oxygen disorder, higher values of dc resistivity, and lower values of $T_c$. This is in agreement with the picture proposed in the work of Ghosh *et al.*[2] on La$_{1-y}$Ca$_y$Mn$_{1-x}$M$_x$O$_3$, suggesting that the local stress produced by the substitutional ion modifies the Mn-O distances around the substitutional ion. This leads to changes of the energies of the $e_g$ orbitals, and to a localization of the itinerant electrons which competes with the DE interaction. Consequently, the JT disorder is enhanced, dc resistivity increases, and $T_c$ decreases. These trends are weaker in the case of Cu substitution although the ionic radius is close to that of Zn and Sc. It is possible that some additional effects due to the electronic or magnetic structure of Cu enhance the mobility of electrons.

The Raman spectra exhibit an additional $A_g$-like mode that we attribute to the local breathing mode of oxygens in a close vicinity of the substituent ion. Its frequency and intensity are very sensitive to the type of substituent. They seem to depend on the position of the substituent ion in the Periodic Table suggesting that the electronic characteristics of the $M$-O bond are important. However, the origin of these effects remains an open question for future studies. The

mode of the Co-substituted samples exhibits an anomalous softening of 15 cm$^{-1}$ when going from 300 to 77 K, which is likely due to the spin state transition of Co.

We believe that our results may be helpful for understanding the electronic properties of manganites, in particular, and transition metal oxides, in general.

*Electronic address: dubroka@physics.muni.cz

†Permanent address: Center for Solid State Physics and New Materials, Institute of Physics, P.O. Box 68, 11080 Belgrade/Zemun, Serbia.

[1] M. B. Salamon and M. Jaime, Rev. Mod. Phys. **73**, 583 (2001).

[2] K. Ghosh, S. B. Ogale, R. Ramesh, R. L. Greene, T. Venkatesan, K. M. Gapchup, Ravi Bathe, and S. I. Patil, Phys. Rev. B **59**, 533 (1999).

[3] K. H. Ahn, X. W. Wu, K. Liu, and C. L. Chien, Phys. Rev. B **54**, 15299 (1996); L. Pi, L. Zheng, and Y. Zhang, *ibid.* **61**, 8917 (2000); Y. Sawaki, K. Takenaka, A. Osuka, R. Shiozaki, and S. Sugai, *ibid.* **61**, 11588 (2000); F. Rivadulla, M. A. López-Quintela, L. E. Hueso, P. Sande, J. Rivas, and R. D. Sánchez, *ibid.* **62**, 5678 (2000).

[4] Z. El-Fadli, M. R. Metni, F. Sapiña, E. Martinez, J. V. Folgado, and A. Beltrán, Chem. Mater. **14**, 688 (2002). Tables of refined structural parameters for the rhombohedral setting are available free of charge at http://pubs.acs.org.

[5] G. De Marzi, H. J. Trodahl, J. Bok, A. Cantarero, and F. Sapiña, Solid State Commun. **127**, 259 (2003).

[6] G. De Marzi, Z. V. Popović, A. Cantarero, Z. Dohčević-Mitrović, N. Paunović, J. Bok, and F. Sapiña, Phys. Rev. B **68**, 064302 (2003).

[7] A. G. Souza Filho, J. L. B. Faria, I. Guedes, J. M. Sasaki, P. T. C. Freire, V. N. Freire, J. Mendes Filho, M. M. Xavier Jr., F. A. O. Cabral, J. H. de Araújo, and J. A. P. da Costa, Phys. Rev. B **67**, 052405 (2003).

[8] J. Vergara, R. J. Ortega-Hertogs, V. Madurga, F. Sapiña, Z. El-Fadli, E. Martínez, A. Beltrán, and K. V. Rao, Phys. Rev. B **60**, 1127 (1999).

[9] O. Chmaissem, B. Dabrowski, S. Kolesnik, J. Mais, J. D. Jorgensen, and S. Short, Phys. Rev. B **67**, 094431 (2003).

[10] J. Blasco, J. García, and J. Stankiewicz, Phys. Rev. B **68**, 054421 (2003).

[11] R. D. Shannon, Acta Crystallogr., Sect. A: Cryst. Phys., Diffr., Theor. Gen. Crystallogr. **32**, 751 (1976); http://abulafia.mt.ic.ac.uk/shannon/ptable.php.

[12] P. G. Radaelli and S.-W. Cheong, Phys. Rev. B **66**, 094408 (2002).

[13] M. V. Abrashev, A. P. Litvinchuk, M. N. Iliev, R. L. Meng, V. N. Popov, V. G. Ivanov, R. A. Chakalov, and C. Thomsen, Phys. Rev. B **59**, 4146 (1999).

[14] E. Granado, N. O. Moreno, A. García, J. A. Sanjurjo, C. Rettori, I. Torriani, S. B. Oseroff, J. J. Neumeier, K. J. McClellan, S.-W. Cheong, and Y. Tokura, Phys. Rev. B **58**, 11435 (1998).

[15] V. B. Podobedov, D. B. Romero, A. Weber, J. P. Rice, R. Schreekala, M. Rajeswari, R. Ramesh, T. Venkatesan, and H. D. Drew, Appl. Phys. Lett. **73**, 3217 (1998).

[16] X. Liu, S. Xu, K. Kato, and Y. Moritomo, J. Phys. Soc. Jpn. **71**, 2820 (2002).

[17] M. N. Iliev and M. V. Abrashev, J. Raman Spectrosc. **32**, 805 (2001).

[18] V. B. Podobedov, A. Weber, D. B. Romero, J. P. Rice, and H. D. Drew, Phys. Rev. B **58**, 43 (1998).

[19] P. Björnsson, M. Rübhausen, J. Bäckström, M. Käll, S. Eriksson, J. Eriksen, and L. Börjesson, Phys. Rev. B **61**, 1193 (2000).

[20] M. N. Iliev, M. V. Abrashev, V. N. Popov, and V. G. Hadjiev, Phys. Rev. B **67**, 212301 (2003).

[21] R. Shuker and R. W. Gammon, Phys. Rev. Lett. **25**, 222 (1970).

[22] M. V. Abrashev, V. G. Ivanov, M. N. Iliev, R. A. Chakalov, R. I. Chakalova, and C. Thomsen, Phys. Status Solidi B **215**, 631 (1999).

[23] A. E. Pantoja, H. J. Trodahl, R. G. Buckley, Y. Tomioka, and Y. Tokura, J. Phys.: Condens. Matter **13**, 3741 (2001).

[24] L. Martín-Carrón and A. de Andrés, Eur. Phys. J. B **22**, 11 (2001).

[25] Zheng Wen-Chen, J. Phys.: Condens. Matter **7**, 4499 (1995).

[26] T. Boix, F. Sapiña, Z. El-Fadli, E. Martinez, A. Beltrán, J. Vergara, R. J. Ortega, and K. V. Rao, Chem. Mater. **10**, 1569 (1998).

[27] L. Martín-Carrón, A. de Andrés, M. J. Martínez-Lope, M. T. Casais, and J. A. Alonso, Phys. Rev. B **66**, 174303 (2002).

[28] K. H. Kim, J. Y. Gu, H. S. Choi, D. J. Eom, J. H. Jung, and T. W. Noh, Phys. Rev. B **55**, 4023 (1997).

[29] J. L. Alonso, L. A. Fernández, F. Guinea, V. Laliena, and V. Martín-Mayor, Phys. Rev. B **66**, 104430 (2002).